Transient photoluminescence enhancement as a probe of the structure of impurity-trapped excitons in CaF$_2$:Yb^{2+}

Michael F. Reid,[1] Pubudu S. Senanayake,[2] Jon-Paul R. Wells,[2,*] Giel Berden,[3] Andries Meijerink,[4] Alexander J. Salkeld,[2] Chang-Kui Duan,[5] and Roger J. Reeves[1]

[1]*Department of Physics and Astronomy and MacDiarmid Institute for Advanced Materials and Nanotechnology, University of Canterbury, PB 4800, Christchurch 8140, New Zealand*
[2]*Department of Physics and Astronomy, University of Canterbury, PB 4800, Christchurch 8140, New Zealand*
[3]*FELIX Free Electron Laser Facility, FOM Institute for Plasmaphysics Rijnhuizen, PO Box 1207, 3430 BE, Nieuwegein, The Netherlands*
[4]*Debye Institute for NanoMaterials Science, University of Utrecht, P.O. Box 80000, TA 3508 Utrecht, The Netherlands*
[5]*Department of Physics, University of Science and Technology of China, Hefei 230026, China*
(Received 15 July 2011; revised manuscript received 23 August 2011; published 23 September 2011)

We demonstrate a direct measurement of the energy levels of impurity-trapped excitons in CaF$_2$:Yb^{2+}. The radically different radiative decay rates of the lowest exciton state and higher excited states enable the generation of a transient photoluminescence enhancement measured via a two-step excitation process. We observe sharp transitions arising from changes of state of localized electrons, broad bands associated with changes of state of delocalized electrons, and broad bands arising from trap liberation.

The unique optical properties of rare-earth doped materials are responsible for their crucial role in a wide variety of applications such as fluorescent tubes, white light LEDs, lasers, fiber amplifiers, and medical imaging.[1,2] The sharp-line optical transitions within the $4f^N$ ($N = 0$–14) ground configurations of rare-earth ions have been extensively studied and may be accurately modeled.[1–3] Transitions involving excited configurations such as $4f^{N-1}5d$ are crucial to many applications, but information about these states is limited because $4f^N \leftrightarrow 4f^{N-1}5d$ spectra consist of broad vibronic bands, yielding much less information than $4f^N \leftrightarrow 4f^N$ spectra.[4–8] Modern *ab initio* methods[9,10] are capable of accurately calculating excited-state electronic structure and bond-length variations, giving good agreement with available broad-band $4f^N \leftrightarrow 4f^{N-1}5d$ spectra. The *ab initio* calculations[10] indicate that transitions *between* the excited states would give a combination of sharp-line and broad vibronic transitions. We have recently proposed that two-frequency excitation experiments would provide more detailed information about the excited states and better test the calculations.[11]

Excited configurations of rare-earth ions are not restricted to $4f^{N-1}5d$. Configurations involving charge transfer between the rare-earth ion and other ions in the material are also important. Theoretical[9] and experimental[12,13] studies suggest that nonradiative relaxation of the $4f^{N-1}5d$ configuration is often mediated by trapped exciton states, where the excited electron is no longer completely localized on the rare-earth ion.

In some Eu^{2+} and Yb^{2+} materials, emission from excitonic states may be observed.[14,15] Excitonic emission in CaF$_2$ and SrF$_2$ doped with Yb^{2+} has been the subject of several studies.[14,16–18] The ground-state electronic configuration of CaF$_2$:Yb^{2+} is $4f^{14}$. UV excitation can promote one of the $4f$ electrons to a $5d$ orbital, giving the excited configuration $4f^{13}5d$. The $5d$ electron rapidly becomes delocalized over the next-nearest-neighbor Ca^{2+} ions. The Yb^{2+} is then effectively ionized to Yb^{3+}, with electronic configuration $4f^{13}$, i.e., one $4f$ *hole*. This trivalent ion attracts the F$^-$ nearest

neighbors more strongly than a divalent ion, leading to a large contraction of bond length. Emission from the exciton states to the $4f^{14}$ ground state involves the reverse change in bond length, and therefore a broad, structureless, red-shifted vibrational emission band.[14,15] Recent *ab initio* calculations have given valuable insight into the quantum physics of exciton formation.[9] However, the broad bands provide no detailed information, and experimental information on the energy-level structure of impurity-trapped excitons is largely deduced from indirect measurements such as temperature dependencies,[16,17] pressure dependencies,[12] and photoconductivity.[18]

In this Brief Report, we report on an investigation of the internal structure of impurity-trapped excitons using two-frequency measurements of single-crystal CaF$_2$ doped with Yb^{2+}. By applying IR radiation to the crystal after exciting it in the UV, we induce transitions between exciton states. Since some of the exciton-excited states have much higher radiative rates than the lowest exciton state, we can detect the excited state absorption by monitoring photoluminescence enhancement.

CaF$_2$:Yb^{2+} crystals were grown using the vertical Bridgmann technique. The UV component of our two-frequency excitation was from a Quantronix TOPAS traveling-wave optical parametric amplifier (OPA) providing 3 ps pulses tunable in the 250–400 nm region of interest in this work at a repetition rate of 1 kHz. Pulsed infrared excitation was achieved using the Dutch free electron laser (FEL) FELIX in Nieuwegein. The IR output of FELIX consists of a 4–6 μs macropulse at a repetition rate of 10 Hz, containing micropulses at 25 MHz. FELIX is continuously tunable from 3 to 250 μm. The OPA was synchronized to the FEL, and the electronic timing between the two lasers could be varied. The UV and IR beams were spatially (but not temporally) overlapped on the sample, held at cryogenic temperatures within an Oxford instruments *microstat* helium flow cryostat. Visible fluorescence was detected using a TRIAX 320 spectrometer equipped with a C31034 photomultiplier. Our results for 365-nm-pulsed UV excitation of CaF$_2$:Yb^{2+} are consistent

with previous work,[16,17] which reported strongly red-shifted fluorescence having a single-exponential decay with a lifetime of 15 ms at 4.2 K that reduces at higher temperatures.

In Fig. 1(a), the fluorescence spectra for CaF_2:Yb^{2+} at 10 K and 40 K are shown. At 10 K, the band center and width

FIG. 1. Fluorescence from CaF_2:Yb^{2+} for excitation at 365 nm. (a) Spectra at 10 K and 40 K 900 μs after UV excitation. (b) Time evolution of 10 K emission spectrum excited with 12.1 μm (826 cm^{-1}) IR radiation following the UV pre-pulse. The asterisk (*) shows a combination of first- and second-order UV scatter and emission from minor Eu^{2+} impurities. (c) Time evolution of 10 K emission spectrum excited with 16 μm (625 cm^{-1}) IR radiation following the UV prepulse. The (b) and (c) insets show the time profile at peak emission wavelength.

(FWHM) are 17720 and 3460 cm^{-1} respectively. At 40 K, the intensity increases by a factor of 2.5 and the band center and width are 18380 and 3240 cm^{-1} respectively. Previous analysis of the temperature dependence[16] suggests that the emission is from two states whose energy separation is about 40 cm^{-1}, with very different radiative lifetimes: 15 ms for the lower state and 260 μs for the upper state.

The shift in band center and change in bandwidth indicate that the two excited states have different bond lengths. Emission bandwidths have been previously used to calculate the change in bond length between the lowest exciton state and the ground state as 0.17 Å,[16] much larger than bond-length changes for transitions between $4f^N$ and $4f^{N-1}5d$ configurations.[7,10] The calculation is approximate because it uses an effective phonon frequency. A frequency of 325 cm^{-1} gives a bond-length change of -0.17 Å for the lowest exciton state relative to the ground state (from our 10 K data) and -0.16 Å for the first excited exciton state (from our 40 K data). The first excited state thus has a *longer* bond length, closer to the ground state $4f^{14}$ bond length.

We now present the results of our two-frequency transient measurements at 10 K. Figures 1(b) and 1(c) show respectively the results of irradiating the system at a wavelength of 12.1 μm (826 cm^{-1}) and 16 μm (625 cm^{-1}), delayed from the UV excitation by 100–200 μs. The application of the IR pulse yields significant *enhancement* of the emission. Note that the IR pulse on its own cannot induce this optical emission. The enhancement occurs because we now populate excited excitonic states that have significantly *higher* radiative rates. An enhancement of the total emission at long time scales is also observed. We interpret this as liberation of electrons from traps (discussed below), which is known to occur under intense IR radiation.[19]

For 12.1 μm IR excitation, there is a rise time of approximately 6 μs, and a decay time of 43 μs. The spectrum at the time corresponding to the maximum emission intensity is similar to the 40 K spectrum in Fig. 1(a). The enhanced emission is therefore likely to be a result of radiation from the state 40 cm^{-1} above the lowest exciton state. Further evidence for this conclusion is that at 40 K the IR excitation gives only a small enhancement and no change to the spectrum. The decay of the transient signal is much faster than the estimated 260 μs radiative lifetime,[16] due to nonradiative processes.[17]

The spectral and temporal behavior for 16 μm excitation [Fig. 1(c)] is very different. The time development cannot be fitted by single exponential rise and decay times, but the rise time is approximately 30 μs and the decay approximately 160 μs. At the time corresponding to the maximum emission intensity, we observe a mixture of low-energy and high-energy Gaussians. Several hundred μs after the IR excitation pulse, the intensity of the low-energy Gaussian is still significantly higher than before the IR pulse, suggesting that there are significantly *more* ions radiating than before the IR excitation.

The range of IR energies for which we have observed enhancement of the visible emission is shown in the excitation spectrum of Fig. 2(a), where the photoluminescence transient is time integrated to give the signal. The spectrum consists of a broad band centered at 650 cm^{-1} and two sharper peaks at 250 cm^{-1} and 1145 cm^{-1}, with linewidths of 35 and 20 cm^{-1} respectively. We note that dips in the broad band and the lower
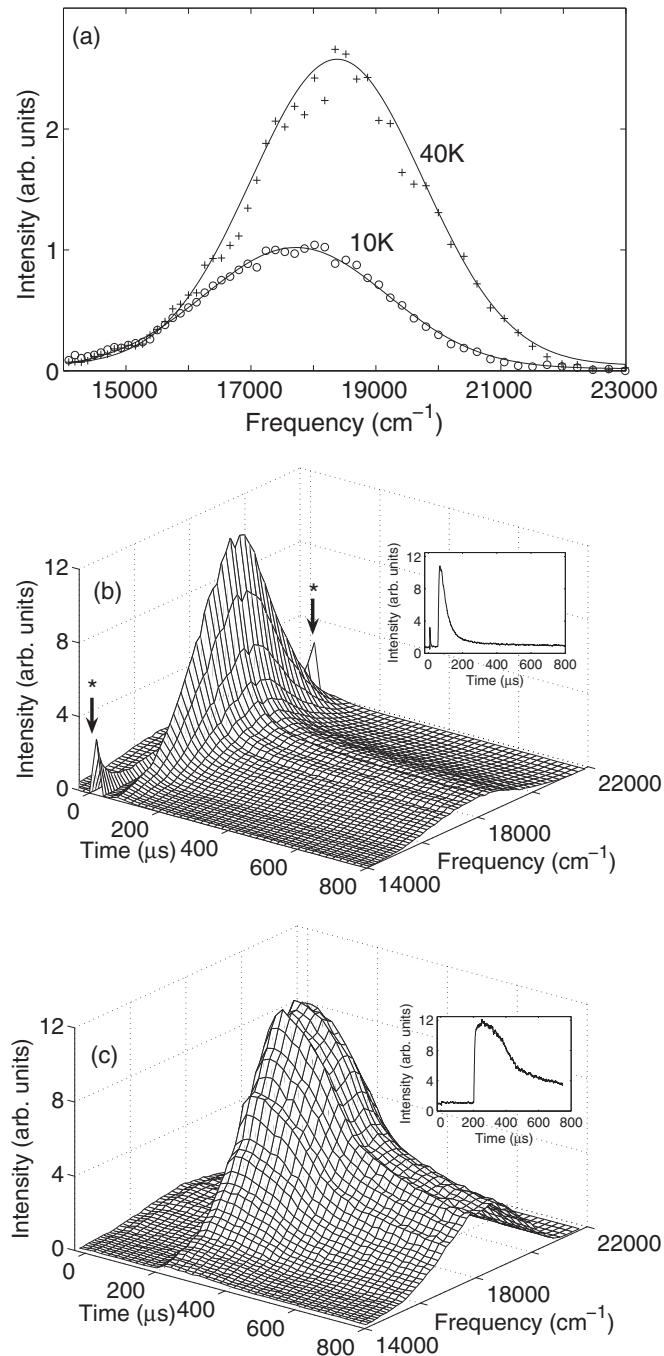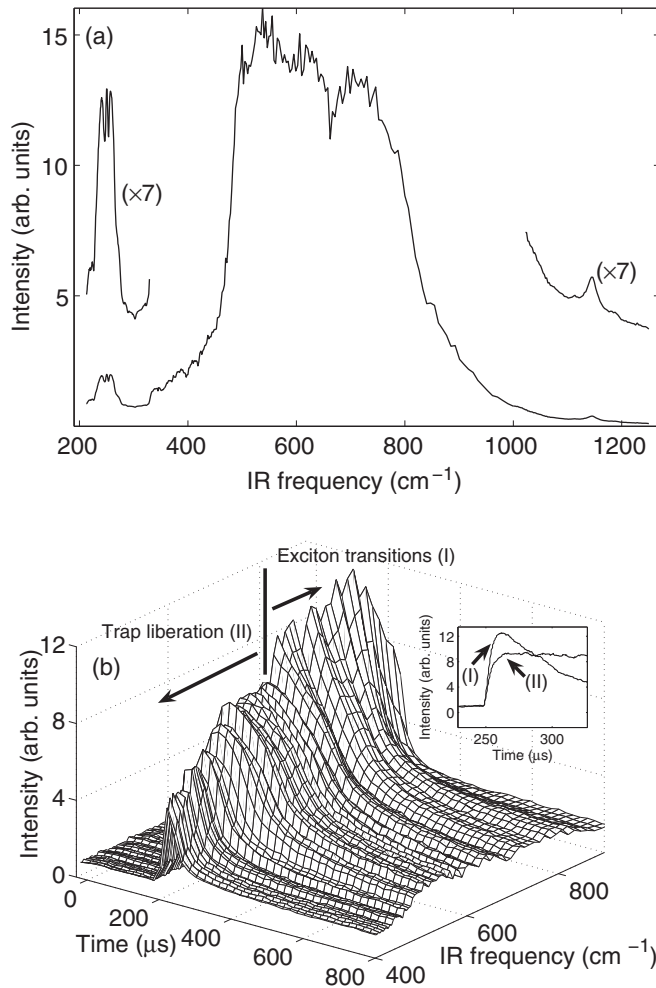
FIG. 2. (a) 10 K IR excitation spectrum of CaF_2:Yb^{2+} deduced by integrating emission enhancement over time. The regions where sharp peaks are observed have been magnified and displaced for clarity. (b) Time evolution of the 10 K IR excitation spectrum. Inset: rise time with (I) IR excitation at 825 cm^{-1}, (II) IR excitation at 625 cm^{-1}.
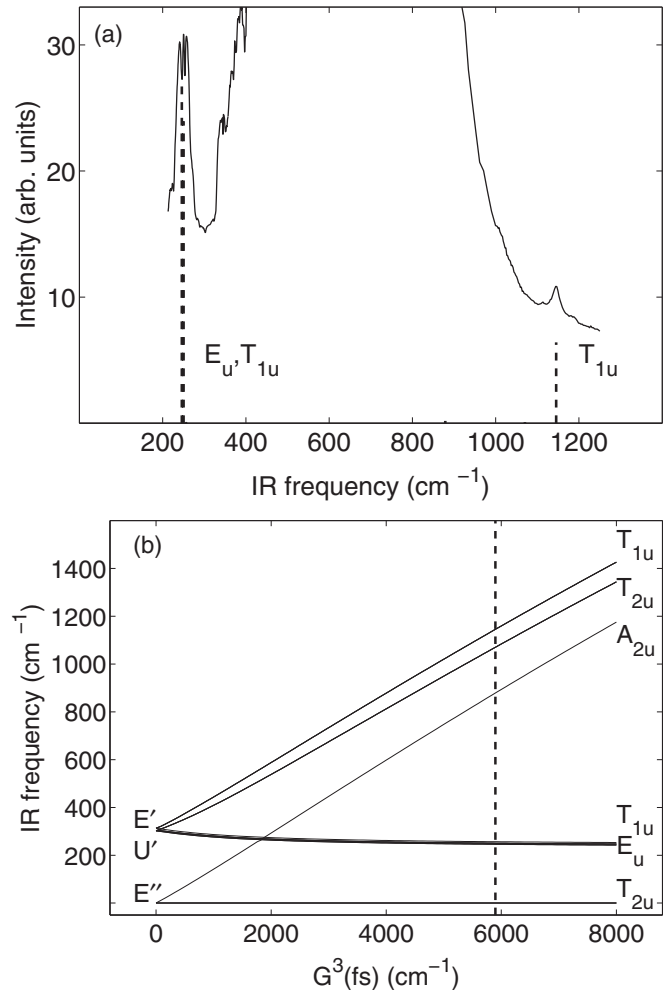

FIG. 3. (a) Calculated oscillator strengths (vertical lines) and experimental IR excitation spectrum. (b) Dependence of the exciton energy levels on the exchange parameter $G^3(fs)$. The vertical dotted line is at the value of $G^3(fs)$ used in the calculation of Fig. 3(a).

sharp peak correlate with atmospheric absorption of the FEL radiation, which can distort the lineshape, despite purging of the IR beam path with dry N_2 gas.

The strong dependence of the temporal dynamics on the IR excitation wavelength is further illustrated in Fig. 2(b). The broad peak is actually two distinct regions, a higher-energy region with fast rise and decay times, and a lower-energy region dominated by slow rise and decay times. We attribute the long-lived signal in this region to trap liberation processes. Whereas transitions within the exciton transfer population from the lowest exciton state to a state with a much higher radiative rate, trap liberation processes increase the total number of excitons radiating. A phenomenological model of a Coulomb trap having a threshold of 380 cm^{-1} gives an asymmetric spectrum with a width of approximately 400 cm^{-1} [Ref. 19, Eq. (3)], which is consistent with the width of the low-energy band.

The high-energy part of the band, from 650 to 950 cm^{-1}, and the sharp lines, are assigned to transitions within the exciton. Recall that our exciton model is a Yb^{3+} ion with one $4f$ hole ($4f^{13}$) and a delocalized electron. It is the

delocalized electron that can affect bonding, so the vibronic broadening of the 650–950 cm^{-1} band leads us to attribute this feature to transitions that change the orbital of the delocalized electron and therefore the bond length. The width of this band is similar to the width of the phonon spectrum in CaF_2,[20] which implies that the bond-length change for the transition is small, similar to the difference in bond length between the lowest two exciton states calculated above (0.01 Å). An accurate calculation of the position and width of this band should be possible with a detailed *ab initio* approach, as in Ref. 9.

The sharp excitation features observed at 250 and 1145 cm^{-1} cannot involve a change in bonding. We therefore assign them to changes in the wave function of the localized $4f$ hole or the relative spin of the $4f$ hole and delocalized electron. The latter is associated with an exchange Coulomb interaction. The calculations of Ref. 9 suggest that the excitons involve a linear combination of $5d$ and $6s$ orbitals with totally symmetric s character. Unlike the $SrCl_2$:Yb^{2+} system,[10] detailed calculations for CaF_2:Yb^{2+} are not available. However, we may model the sharp lines with a simple semiempirical

model by constructing a "crystal field" Hamiltonian for an s electron and a $4f$ hole in a cubic crystal field,

$$H_{\text{cf}} = \zeta A_{\text{so}} + B^4 \left(C_0^4 + \sqrt{\frac{5}{14}} [C_4^4 + C_{-4}^4] \right)$$
$$+ B^6 \left(C_0^6 - \sqrt{\frac{7}{2}} [C_4^6 + C_{-4}^6] \right) + G^3(fs)g_3(fs), \quad (1)$$

where ζ is the spin-orbit interaction for the $4f$ electrons, B^4 and B^6 are crystal-field parameters for the $4f$ electrons, and $G^3(fs)$ is the exchange interaction between the $4f$ and the delocalized electron. Details of the Hamiltonian operators may be found in Refs. 3,4,6,8,21.

Since we only observe two sharp lines, it is not possible to fit all of the parameters in Eq. (1). The spin-orbit parameter ζ was fixed at 2928 cm^{-1}, the value determined for Yb^{3+} in LaF$_3$.[3] The ratio B^6/B^4 was fixed at -0.35, the value obtained by Leśniak[22] for Er^{3+} in CaF$_2$. With these assumptions, the parameter values $B^4 = -800$ cm^{-1} and $G^3(fs) = 5900$ cm^{-1} give energy levels that match the observed sharp lines.

Figure 3 illustrates our calculation. When the $G^3(fs)$ parameter is set to zero, the $^2F_{7/2}$ multiplet of $4f^{13}$ splits into E'', U', and E' irreducible representations of the octahedral group,[23] as illustrated on the left side of Fig. 3(b). As $G^3(fs)$ is increased, these states couple with ^2S (from the s electron). In cubic symmetry, only magnetic-dipole transitions are allowed. Calculated absorption oscillator strengths are compared with experiment in Fig. 3(a). Note that several transitions are forbidden or calculated to be very small.

The B^4 parameter is similar to the value of -725 cm^{-1} for the $4f^{13}5d$ configuration of Yb^{2+} in SrCl$_2$.[8] A Hartree-Fock calculation using the atomic code of Cowan[21] gives $G^3(fs) = 3167$ cm^{-1} for the $4f^{13}6s$ configuration of Yb^{2+}. This is smaller than our experimental value. However, the calculations of Ref. 9 suggest that the exciton will contain mixtures of $5d$ and $6s$ orbitals. The exchange splitting for $4f^{13}5d$ is over 2000 cm^{-1},[8] so our observed splitting of about 1145 cm^{-1} for the exciton, where the electron is in a more delocalized orbital than $5d$, is reasonable.

In conclusion, we have demonstrated that it is possible to probe the internal structure and dynamics of exciton states, and trap-liberation processes, in rare-earth materials with a two-frequency selective fluorescence enhancement technique. We observe sharp-line transitions within the exciton spectrum. A quantitative account of these sharp line features has been obtained using a parametrized crystal-field model. Our observations provide a basis and motivation for detailed *ab initio* calculations as in Ref. 9 and for investigation of other rare-earth excitonic systems using the same experimental approach.

*Corresponding author: jon-paul.wells@canterbury.ac.nz

[1]*Properties of Rare Earths in Optical Materials*, edited by G. K. Liu and B. Jacquier (Springer, Berlin, 2005).

[2]*Luminescence: From Theory to Applications*, edited by C. Ronda (Wiley-VCH, Weinheim, 2007).

[3]W. T. Carnall, G. L. Goodman, K. Rajnak, and R. S. Rana, J. Chem. Phys. **90**, 3443 (1989).

[4]L. van Pieterson, M. F. Reid, R. T. Wegh, S. Soverna, and A. Meijerink, Phys. Rev. B **65**, 045113 (2002).

[5]L. van Pieterson, M. F. Reid, G. W. Burdick, and A. Meijerink, Phys. Rev. B **65**, 045114 (2002).

[6]G. W. Burdick and M. F. Reid, in *Handbook on the Physics and Chemistry of the Rare Earths*, Vol. 37, edited by K. A. Gschneidner Jr., J. C. Bunzli, and V. K. Percharsky (Elesevier, North Holland, 2007), Chap. 232, pp. 61–91.

[7]M. Karbowiak, A. Urbanowicz, and M. F. Reid, Phys. Rev. B **76**, 115125 (2007).

[8]Z. Pan, C. K. Duan, and P. A. Tanner, Phys. Rev. B **77**, 085114 (2008).

[9]G. Sánchez-Sanz, L. Seijo, and Z. Barandiarán, J. Chem. Phys. **133**, 114509 (2010).

[10]G. Sánchez-Sanz, L. Seijo, and Z. Barandiarán, J. Chem. Phys. **133**, 114506 (2010).

[11]M. F. Reid, L. Hu, S. Frank, C. K. Duan, S. Xia, and M. Yin, Eur. J. Inorg. Chem. **2010**, 2649 (2010).

[12]M. Grinberg and S. Mahlik, J. Non-Cryst. Solids **354**, 4163 (2008).

[13]S. Mahlik, M. Grinberg, E. Cavalli, M. Bettinelli, and P. Boutinaud, J. Phys.: Condens. Matter **21**, 105401 (2009).

[14]D. S. McClure and C. Pedrini, Phys. Rev. B **32**, 8465 (1985).

[15]P. Dorenbos, J. Phys. Condens. Matter **15**, 2645 (2003).

[16]B. Moine, B. Courtois, and C. Pedrini, J. Phys. **50**, 2105 (1989).

[17]B. Moine, B. Courtois, and C. Pedrini, J. Lumin. **48-49**, 501 (1991).

[18]C. Pedrini, M. F. Joubert, and D. S. McClure, J. Lumin. **125**, 230 (2007).

[19]I. Izeddin, M. A. J. Klik, N. Q. Vinh, M. S. Bresler, and T. Gregorkiewicz, Phys. Rev. Lett. **99**, 077401 (2007).

[20]W. Hayes, M. C. K. Wiltshire, W. J. Manthey, and D. S. McClure, J. Phys. C **6**, L273 (1973).

[21]R. D. Cowan, *The Theory of Atomic Structure and Spectra* (U. California, Berkeley, 1981).

[22]K. Leśniak, J. Phys. Condens. Matter **2**, 5563 (1990).

[23]B. Henderson and G. F. Imbusch, *Optical spectroscopy of inorganic solids* (Clarendon Press, Oxford, 1989).